The Prediction of Side Force and Yaw Moment for Sailing Yacht Hulls

Abstract. Side Force and Yaw Moment are predicted based on first principles and on corrections, derived from a regression analysis of towing tank tests data. The results are used in a VPP computer program.

NOMENCLATURE

AR_{geo}	geometric aspect ratio
AR_{eff}	effective aspect ratio
B_{WL}	maximum beam in the water plane, heeled
c	chord length of foil
C_m	area coefficient of main section
C_M	coefficient of the free Munk-moment
C_P	prismatic coefficient
Fn	Froude number if based on chord length c $= U_\infty / (g \cdot c)^{1/2}$
g	gravitational acceleration = 9.81 m/s^2
L_{WL}	length of the actual water line at heel
q	dynamic pressure = ½ ρ U_∞^2
T_{Lat}	max. lateral draft of canoe body, heeled
T_{CB}	max. draft of canoe body, upright
T_{Rud}	rudder span (draft)
U_∞	boat speed
V_{CB}	volume of canoe body
δ	leeway angle
γ	angle between x-axis and line of deepest draft
φ	heel angle
ψ	pitch angle, bow up positive
ρ	mass density

1. INTRODUCTION

In a previous analysis [1] the effects of leeway and rudder angle on the resistance of sailing yacht hulls were reported. The investigation is extended in this paper on the prediction of the side force and the yaw moment. The predictions are compared to towing tank data of 6 models of the Delft Systematic Yacht Hull Series [2] and of the models #4-9 of the USSAIL-series [3]. In the DSYHS the appendages carried sand strips as a boundary-layer trip very close to the leading edge. From wind-tunnel tests with sandpaper applied to the leading edge of an airfoils [4] it is known, that the drag increases significantly, but the lift coefficient remains almost unchanged up to the separation point. The separation occurs much earlier than on the clean profile. Therefore only tank runs with leeway < 9° were used for the comparison.

2. THE GENERATION OF SIDE FORCES

The submerged part of the sailing yacht needs to generate a side force to counterbalance the side force that is generated by the sails. This side force on the hull is proportional to the leeway, i.e. the angle between the direction of travel and the centreline of the hull. It is the sum of the forces generated by the keel, the rudder and the canoe body. The theory of the airplane can be applied to the modern keel and rudder, and the side force is equivalent to the lift of wing and elevator.

2.1 Side forces of keel and rudder

The lift and drag characteristics of a hydrofoil section are either known from wind-tunnel tests [5] or can be calculated with the program XFOIL [6] as a function of the angle of attack and the Reynolds-number. Tables of lift and drag coefficients for several profiles that are often used in keel- and rudder-design were prepared for the computer program. Polynomials of higher order are used for interpolation. The actual lift and drag of the keel is determined by integrating the forces on 8 different sections along the span of the fin. This division of the span allows a wide variation of thicknesses and plan forms. The effect of the finite span, which is a function of the aspect ratio, is computed using Küchemann's method [7]. For large angles of attack and foils with a sharp tip, the lift coefficient is increased by a quadratic increment. Lamar's side edge suction analogy [8] predicts this increment. If there is a ballast bulb at the tip of the keel, no vortex will create a suction force. Instead the bulb will act as an endplate. The influence of the endplate on the lift distribution along the span is described in [9]. A large impact has the presence of the hull; it changes the flow around the keel significantly. The method of conformal mapping, as described by Johanna Weber [10], allows calculating the interaction between keel and hull. This transformation yields as result the change of the flow speed over the keel and therefore the change in lift created by the keel. The forces on the rudder are calculated in a similar manner, based on average values for chord and thickness. The downwash behind the keel, which changes the angle of attack for the rudder, is calculated using Hoerner's equations [11].

2.2 Side force generated by the hull

There are two different ways in which the hull can generate a side force. First, the hull alone, without appendages will experience a side force under leeway. The hull can be regarded as a lifting body with a very small aspect ratio. In this case the method of R. T. Jones [11] will give a first approximation of the side force. The method is valid for wings with defined leading edges. The force will be reduced on a round bottomed hull. A correction factor is therefore applied, depending on the sharpness of the forebody.

A second source of side force is the carry over of the pressure field generated by the keel onto the hull. This pressure field on the hull results in an additional side force. Johanna Weber [10] proposes a method to calculate the force on the fuselage of an airplane, which is directly comparable to this force on the hull.

2.3 Influence of heel

When the yacht heels, the pattern of the water lines changes. In figure 1 it can be seen, that the line that connects the deepest draft on the bow with the one on the stern moves away from the centerline (x-axis). The angle γ increases with heel.

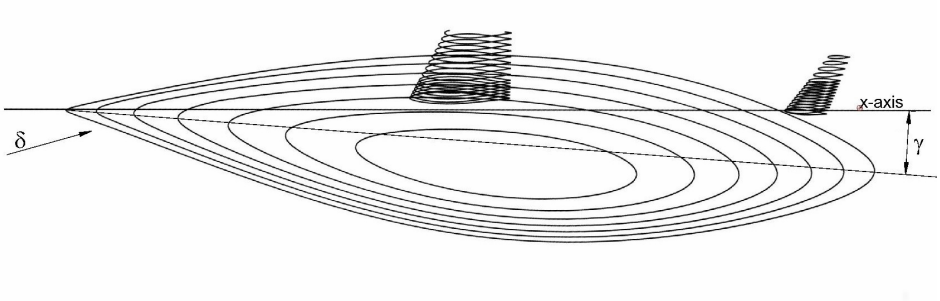

Figure 1. water lines of USSAIL #5 at 25° heel, vertical view to water surface

The lift produced by keel and hull and its interference depend on the angles of attack. With the leeway angle δ the keel sees an angle of attack of $\delta \cdot \cos \varphi$ whereas for the hull the shift of the water lines acts like an additional angle of attack and the effective angle is $\delta + \gamma$.

One can also see in figure 1, that the position of the rudder is not behind the deepest part of the hull any more. If we assume, that the streamlines on the hull surface follow mainly the water lines, then the flow in the upper part of the rudder comes from the "wrong" direction. Binns et al. [12] discovered that with certain hull forms, the total lift of the rudder can even become negative. The VPP contains therefore a correction that is subtracted from the geometric rudder angle. This correction depends on γ, T_{CB}/T_{Rud}, T_{Lat}/B_{WL}, C_m , on the Froude-number and on the position of the rudder, relative to the aft end of the waterplane. A regression analysis of the tank data is used to determine an equation for the angle-correction.

2.4 Influence of the free surface

The big difference between the flow described by airplane theory and the flow around the hull of a yacht is the influence of the free surface of the water plane. Experiments with surface piercing NACA foils without a hull are reported in [13]. Van den Brug et al. tested a vertical flat plate [14]. A helpful parameter is the relation between the effective and the geometric aspect ratio. AR_{eff} is the aspect ratio that must be used in the equation from wing theory [11] to match the measured slope of the lift coefficient. Figure 2 depicts the calculated ratio from the test results for different geometries and Froude-numbers.

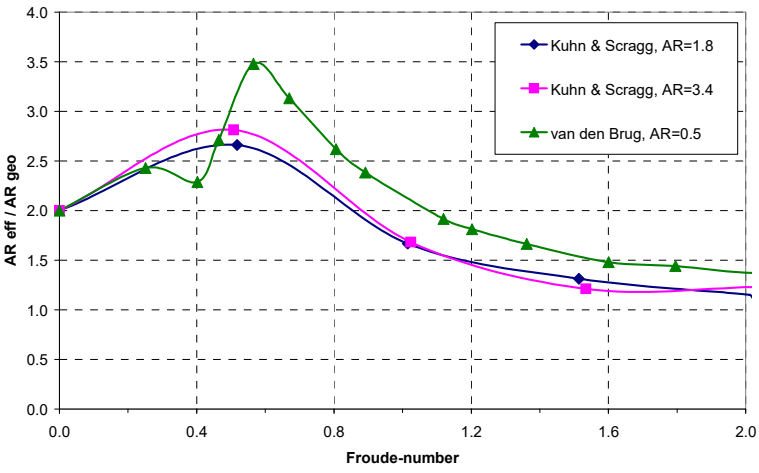

Figure 2. Effective aspect ratio of surface piercing foils and a flat plate, tested in towing tank Froude-number based on chord

At rest (Fn = 0) the water plane acts like a hard mirror and the aspect ratio is doubled. At very high Froude-numbers the water surface is "soft" and the pressure difference across the foil vanishes close to the water surface. In this case, the effective aspect ratio equals the geometric ratio. The effective ratio of the NACA-foils depends obviously only on the Froude-number. The flat plate tested by van den Brug had a very small AR_{geo} and experienced most likely some ventilation.

The keel of a yacht has no direct contact with the water surface; it is shielded by the hull. The bottom of the hull can act like a reflection plane, if it is flat, or level out the pressure differences, if there is a significant deadrise angle. The relation AR_{eff}/AR_{geo} can only be determined from experiments. Figure 3 shows the results from 579 tank runs. The Froude-number is based on the waterline length of the hull. The magenta curve is taken from figure 2.

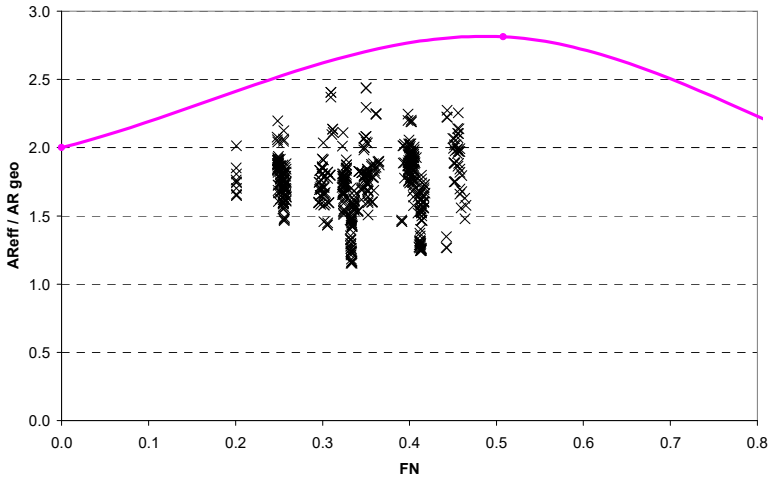

Figure 3. Effective aspect ratio of the tank models dependent on Froude-number, based on L_{WL}

It seems that the curve for the surface piercing foil is the limiting value and the hull acts like a reflection plane, but not as strong as the water surface. A regression analysis of the tank runs yielded an equation for AR_{eff}/AR_{geo} that depends on Fn, C_P, T_{Lat}/L_{WL}, $V_{CB}^{1/3}/L_{WL}$, and deadrise.

2.5 Influence of pitch angle

If the yacht is heeled and travels with a pitch angle, the appendages will be inclined to the incoming flow and this angle of attack creates a side force, even for zero leeway. For accurate predictions an estimate of the pitch angle must be included into the analysis. Let $\boldsymbol{\varphi}$ be the heel angle, $\boldsymbol{\delta}$ the leeway angle and $\boldsymbol{\psi}$ the pitch angle, then the angle of attack for the appendages is:

$$AoA = \delta \cdot \cos\varphi + \psi \cdot \sin\varphi$$

3. THE YAW MOMENT

The side forces that are listed in the previous chapter create all a yaw moment around the origin of the coordinate system. If the center of effort for each force is known, the moment can be calculated. The coe for keel and rudder is the quarter-chord-point; the hull force (Jones) acts a small distance in front of the leading edge of the keel. The sum of these moments does not completely match the moment that was measured in the towing tank tests. According to Munk, every streamlined body has an unstable "free" moment [11]. Due to viscosity effects this moment does not follow the theoretical value. There are two possible ways to define a coefficient for the free moment:

$$C_M = M_{free} \Big/ q \cdot V_{CB} \quad \text{or} \quad C_M = M_{free} \Big/ q \cdot T_{Lat}^{\,2} \cdot L_{WL}$$

When correlating experimental values, the optimum choice depends on the geometry of the body. For the correlation of the towing tank tests it turned out, that it is best to use both versions and split the free moment into two components. Each coefficient C_M is determined by a regression analysis of the tank data and the coefficients depend on $\boldsymbol{\delta}$, $\boldsymbol{\gamma}$, Fn, C_P, $V_{CB}^{1/3}/L_{WL}$ and c/L_{WL}.

4. RESULTS

The prediction is compared to measurements of a model of the yacht Dehler 33 in the towing tank of the SVA Potsdam [15]. This model was not included in the regression analysis. The dimensions of the model are half of

the full size and the model is equipped with load cells at the keel and the rudder. In this way it is possible to check not only the predicted total side force of the yacht but also the individual contributions of keel and rudder. The comparison is depicted in figure 4.

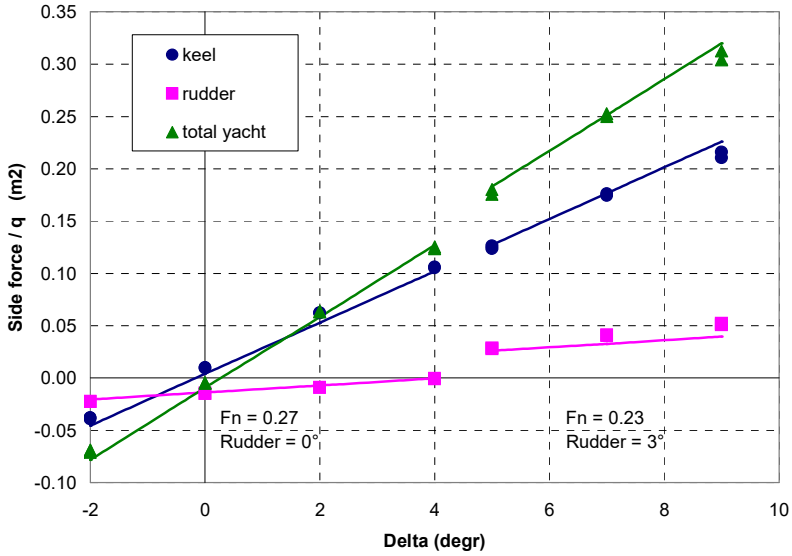

Figure 4.
Side force for Dehler 33 at 12° heel
symbols = experimental data
lines = prediction

There are two groups of measurement, one without rudder deflection and one, at a slightly smaller Froude-number (based on L_{WL}), with the rudder deflected to 3°. The agreement is mostly good. The results at 24° heel (not shown here) are not quite as good, because the side force of the rudder is over predicted which would lead to an error of 1° for the rudder angle in the VPP in this case. All other predictions, forces and the trimmed attitude of the yacht would be correct, only the numerical value of the rudder angle would be 1° off. This is in line with the regression analysis, which yielded a two-sigma-band of 1.5° for the accuracy of the rudder correction.

The yaw moment of the Dehler 33 is not available. Figure 5 shows the total yaw moments of USSAIL#5 and #9. The selected test runs are for Fn = 0.25 and at 25° heel. These are conditions that are difficult to predict. The deviation for #9 is typical of a "bad" prediction. The error for example at 5° leeway would mean that the predicted position of the center of effort of the side force is wrong by 2% of L_{WL}. When the VPP is used to calculate the balance of the yacht and to determine the best mast position, then the recommended mast position would be erroneous by these 2%. Alternatively, if the mast position is not moved, the VPP would predict a weather-helm, that is 1° too large.

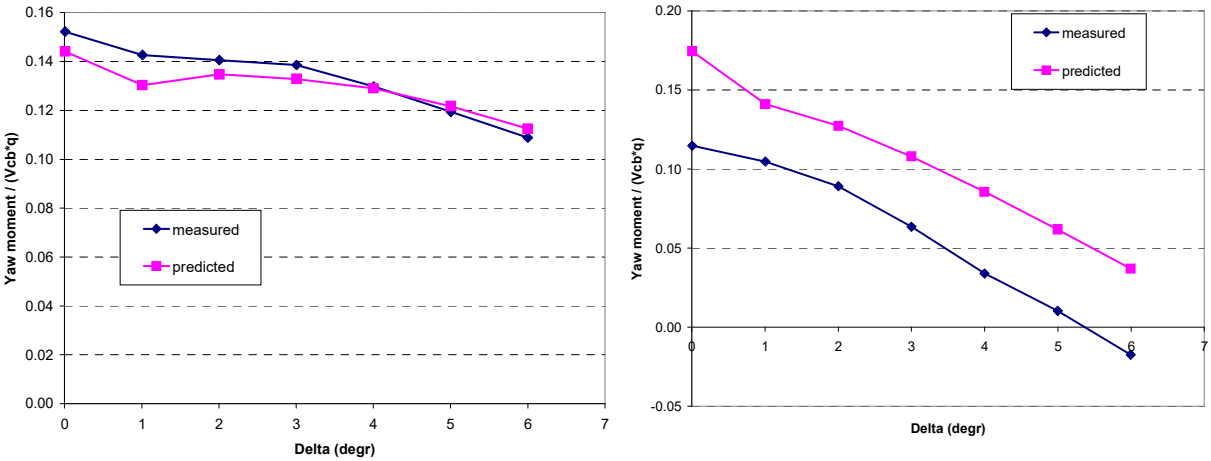

Figure 5. yaw moment USSAIL #5 **yaw moment USSAIL #9**

5. CONCLUSION

The goal for the calculation of forces and moments was to use first principles and the proven airplane theories as much as possible and limit the number of empirical parameters. In the end, three parameters are needed and they were determined by regression analysis of the tank data. One parameter describes the relation between geometric

and effective aspect ratio, one a rudder correction and one the free moment. The accuracy of the prediction is limited by a similarity to the towing tank models. For hull geometries that are significantly different from the tank models, the regression equations have to be extrapolated. The hull of a Class 40 yacht would be such a case and the results should be checked for plausibility. When calculating the balance of the yacht, the accuracy of the predicted rudder angle is ± 2° in the worst case. The described method is used in the VPP UliSpeed. The software can be downloaded from my website [16].

6. REFERENCES

1. Remmlinger, U., "Resistance Prediction for Sailing Yachts, Appended with Leeway, Based on a Regression Analysis of Towing Tank Tests", [Online]. Available: https://www.remmlinger.com/Resistance%20appended+heeled+leeway.pdf
2. http://dsyhs.tudelft.nl/Manual%20DSYHS.pdf
3. Teeters, J., Pallard, R., Muselet, C., "US Sailing Nine Model Series", 2003, not any more available, see: https://www.remmlinger.com/9%20model%20series.zip
4. Broeren, A., Bragg, B., Addy, H., "Effect of Intercycle Ice Accreations on Airfoil Performance", *J. Aircraft*, Vol. 41,No. 1, pp 165-174, 2004,
5. Abbott, I.H., v. Doenhoff, A.E., *Theory of Wing Sections*, New York, USA: Dover, 1959
6. Drela, M., Youngren, H., XFOIL Computer Program, [Online]. Available: http://web.mit.edu/drela/Public/web/xfoil/
7. Küchemann, D., "A Simple Method for Calculating the Span and Chordwise Loading on Straight and Swept Wings of any Given Aspect Ratio at Subsonic Speeds", Aeronautical Research Council, R.&M. No. 2935, 1956
8. Lamar, J., "Extension of Leading-Edge-Suction Analogy to Wings With Separated Flow Around The Edges at Subsonic Speeds", NASA TR R-428, 1974
9. Küchemann, D., Kettle, D.J., "The Effect of Endplates on Swept Wings", Aeronautical Research Council, C.P. No. 104, 1952
10. Weber, J., Kirby, D.A., Kettle, D.J., "An Extension of Multhopp's Method of Calculating the Spanwise Loading of Wing-Fuselage Combinations", Aeronautical Research Council, R.&M. No. 2872, 1956
11. Hoerner, S., *Fluid-Dynamic Lift*, published by Hoerner, L. and v.Borst, H., 1985
12. Binns, J., Klaka, K., Dovell, A., "Hull-Appendage Interaction of a Sailing Yacht, Investigated with Wave-Cut Techniques", *13th Chesapeake Sailing Yacht Symposium*, pp 195-210, 1997
13. Kuhn, J., Scragg, C., "Analysis of Lift and Drag on a Surface-Piercing Foil", *11th Chesapeake Sailing Yacht Symposium*, pp 277-288, 1993
14. van den Brug, J.B., Beukelman, W., Prins, G.J., "Hydrodynamic Forces on a Surfaces Piercing Flat Plate", Shipbuilding Laboratory, Delft University of Technology, Report No. 325, 1971
15. Fröhlich, M., "Optimierung von Kielen einschließlich Rumpf für Segelyachten auf der Basis eines numerischen Rechenverfahrens für viskose und instationäre Strömung", Schiffbau-Versuchsanstalt Potsdam, Germany, 1997
16. https://www.remmlinger.com/UliSpeed.html